Journal of South American Earth Sciences 95 (2019) 102265

Contents lists available at ScienceDirect

Journal of South American Earth Sciences

journal homepage: www.elsevier.com/locate/jsames

Evaluating the feasibility of using Sentinel-2 imagery for water clarity assessment in a reservoir

Matias Bonansea[a,b,*], Micaela Ledesma[b], Raquel Bazán[c], Anabella Ferral[d], Alba German[d,e], Patricia O'Mill[c,e], Claudia Rodriguez[b], Lucio Pinotti[a,f]

[a] Instituto de Ciencias de la Tierra, Biodiversidad y Sustentabilidad Ambiental (ICBIA), Consejo Nacional de Investigaciones Científicas y Técnicas (CONICET), Argentina
[b] Departamento de Estudios Básico y Agropecuarios, Facultad de Agronomía y Veterinaria (FAyV), Universidad Nacional de Río Cuarto (UNRC), Argentina
[c] Departamento de Ingeniería Química y Aplicada, Facultad de Ciencias Exactas Físicas y Químicas, Universidad Nacional de Córdoba (UNC), Argentina
[d] Instituto de Altos Estudios Espaciales Mario Gulich, Centro Espacial Teófilo Tabanera, Comisión Nacional de Actividades Espaciales (CONAE), Argentina
[e] Administración de Recursos de Recursos Hídricos (APRHI), Ministerio de Servicios Públicos, Provincia de Córdoba, Argentina
[f] Departamento de Geología, Facultad de Ciencias Exactas, Físico-Químicas y Naturales, UNRC, Argentina

ARTICLE INFO

Keywords:
Aquatic system
Remote sensing
Statistical algorithm
Sentinel-2 mission
Water quality

ABSTRACT

The new Sentinel-2 satellites present a significant scientific opportunity for the study of water quality. The objective of this study was to evaluate the suitability of Sentinel-2 imagery for estimating and mapping Secchi disk transparency (SDT) in Río Tercero reservoir (Córdoba-Argentina). Field observations and a dataset of atmospherically corrected Sentinel-2 images were used to generate and validate an algorithm to estimate water clarity in the studied reservoir. As a real application of the used methodology, the validated algorithm was used to obtain a spatial representation of water clarity in the reservoir during sampling campaigns. Results demonstrate capabilities of Sentinel-2 mission to make a substantial contribution to the current assessment and understanding of aquatic systems by estimating and mapping a water quality characteristic.

1. Introduction

Lakes and reservoirs have important functions in the environment. Like many other ecosystems, these environments are threatened by the synergistic effects of multiple co-occurring environmental pressures, including human activities, nutrient enrichment, inorganic and organic pollution, and climate change (Palmer et al., 2015; Dörnhöfer and Oppelt, 2016; Ferral et al., 2017; El-Serehy et al., 2018). Therefore, it is imperative to develop new water quality monitoring tools for an efficient management of water resources (Wang et al., 2017).

Satellite remote sensing can improve water quality monitoring and increase the rapid detection of environmental threats, such as eutrophication or harmful algal blooms, due to its time- and cost-effectiveness over large areas as well as remote locations. This is of special interest in the Caribbean and South America region, where there are difficulties in obtaining basic information on water quality (Matthews, 2011; González-Márquez et al., 2018). Furthermore, during the last few years, there is an increasing international interest on the new generation of medium resolution (10–30 m) Earth observation satellites to open a complete new era in the remote sensing of inland waters (Concha and Schott, 2016; Dörnhöfer and Oppelt, 2016; Sovdat et al., 2019). Among these new satellites, the Sentinel-2 mission, developed by the European Space Agency's (ESA) Copernicus program, provides improved continuity for Landsat and SPOT observations and improves data availability for users since it can be used to support global land services including monitoring vegetation, soil and aquatic systems (Drusch et al., 2012; Du et al., 2016; Wang and Atkinson, 2018).

The Sentinel-2 mission carries a push-broom MultiSpectral Instrument (MSI) aboard Sentinel-2A and Sentinel-2B twin satellites which were launched on 23 June 2015 and 7 March 2017, respectively (Sola et al., 2018). The Sentinel-2 mission presents high spatial resolution, multiple spectral bands, short revisit times, and an open data policy, which has made it a rich satellite data archive available to the general public (Sovdat et al., 2019). The pair of Sentinel-2 satellites presents a significant scientific opportunity for the study of aquatic ecosystems by monitoring and mapping water quality constituents in near shore coastal and inland waters. However, Sentinel-2 derived-products require further community-wide validations to ensure performance under different environmental conditions.

The objective of this study was to evaluate the suitability of Sentinel-2 imagery for estimating and mapping Secchi disk transparency (SDT) in Río Tercero reservoir (Córdoba-Argentina). We focused

* Corresponding author. Ruta Nacional Nº 36 Km 601, (5800) Río Cuarto, Córdoba, Argentina.
E-mail address: mbonansea@ayv.unrc.edu.ar (M. Bonansea).

https://doi.org/10.1016/j.jsames.2019.102265
Received 9 May 2019; Received in revised form 4 July 2019; Accepted 5 July 2019
Available online 09 July 2019

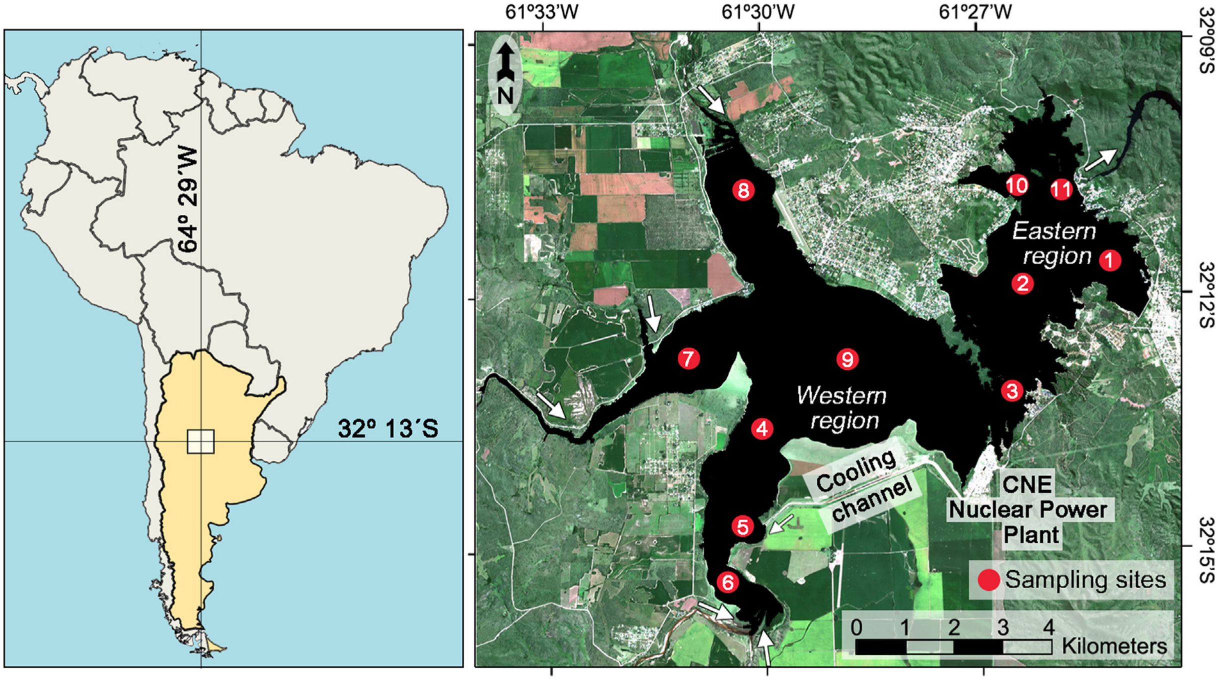

Fig. 1. Study area and location of sampling sites.

on SDT, a common measurement of water clarity, since it is a widely used metric of lakes and reservoirs water quality closely associated with water quality indicators such as trophic status, chlorophyll-a, lake productivity and total phosphorus (Carlson, 1977; Olmanson et al., 2016; Shang et al., 2016). Further, due to its simplicity and low-cost facilities, SDT is commonly used by many volunteer monitoring programs and it is one of the most widely water quality characteristic estimated by remote sensing (Kloiber et al., 2002; Olmanson et al., 2008).

2. Methodology

2.1. Study area

The Río Tercero reservoir is located in the province of Córdoba (Argentina) (Fig. 1). This reservoir has an area of 46 km^2, a volume of 10 hm^3, a maximum and mean depth of 46.5 and 12.2 m respectively (Mariazzi et al., 1992). The Río Tercero reservoir is divided in two regions by a strait. The western region has three branches where rivers flow, while the eastern region presents the only effluent called Tercero river. The Río Tercero reservoir is one of the most important artificial reservoirs in the central region of Argentina since it plays an important ecological and socio-economical role in the development of cities and towns located nearby. In this sense, the studied reservoir has multiple purposes, such as water supply for approximately 20,000 inhabitants, power generation, flood control, irrigation, tourism and recreational activities (Mariazzi et al., 1992). However, in the last two decades, water quality of the reservoir is declining, reducing its multi-purpose value (Bonansea et al., 2016). In 1986 a nuclear power plant (CNE: 600 MWa) was installed. Water for cooling the nuclear reactor is taken from the middle section of the reservoir and is returned to the western basin by a 5 km long open-sky channel (Bonansea et al., 2015). In 2015, the power plant was stopped since it is in a reconditioning process to extend its useful life.

2.2. Field campaigns

Sampling campaigns were conducted on February 28, 2018; March 14, 2018; August 28, 2018; October 17, 2018; February 14, 2019; and March 24, 2019 at eleven sampling sites (Fig. 1). Coordinates of sample sites were recorded using a GPS device. Water clarity was measured using a standard 20 cm diameter Secchi disk from the shady side of a boat to avoid any undesirable effects of water surface reflection. One-way analysis of variance (ANOVA) was performed as a first approach to compare the significant spatial and temporal variation of SDT values measured in the reservoir ($p < 0.05$; least significance difference, LSD).

2.3. Remote sensing data and processing

In the present study, the used remote sensing data was acquired by Sentinel-2A and B satellites. As we have previously mentioned, the Sentinel-2 satellites carry the MSI sensor which measures the reflected solar spectral radiance in thirteen spectral bands ranging from the visible (VIS) to the shortwave infrared (SWIR) bands at 3 different spatial resolutions (Table 1). The radiometric resolution of MSI sensor is 12-bit and it incorporates three new red edge spectral bands (RE1, RE2, RE3) which would improve the accuracy of estimating various biophysical variables (Drusch et al., 2012; Traganos and Reinartz, 2018).

Synchronous to fieldwork activities, cloud-free Sentinel-2A/B images of the study area were downloaded from the USGS Global

Table 1
Band specifications for Sentinel-2 MSI sensor.

Band	Spatial resolution (m)	Wavelength (nm)
1- Aerosol	60	433–453
2- Blue	10	458–523
3- Green	10	543–578
4- Red	10	650–680
5- Red edge (RE) 1	20	698–713
6- RE2	20	733–748
7- RE3	20	773–793
8- Near infrared (NIR)	10	785–900
8a- Near infrared narrow (NIRn)	20	855–875
9- Water vapour	60	935–955
10- Shortwave infrared (SWIR)/ Cirrus	60	1360–1390
11- SWIR-1	20	1565–1655
12- SWIR-2	20	2100–2280

Table 2
Sampling dates and basic statistics of water clarity measured in Río Tercero reservoir.

Sampling campaign	Acquisition image date	Difference in days	SDT values	
			Mean ± Sd.	Range
February 28, 2018	March 1, 2018	1	2.00 ± 0.74	0.50–3.00
March 14, 2018	Mach 14, 2018	0	1.83 ± 0.64	0.75–2.50
August 28, 2018	August 28, 2018	0	1.93 ± 0.86	0.60–3.25
October 16, 2018	October 17, 2018	1	1.83 ± 0.81	0.50–2.90
February 14, 2019	February 14, 2019	0	1.60 ± 0.74	0.60–2.50
March 24, 2019	March 24, 2019	0	2.12 ± 0.81	0.75–3.25

Sd.: Standard deviation.

Visualization Viewer (http://glovis.usgs.gov). Six images acquired on March 1, 2018; Mach 14, 2018; August 28, 2018; October 16, 2018; February 14, 2019; and March 24, 2019 were downloaded as Level-1C products. Level-1C data corresponds to Top-Of-Atmosphere (TOA) reflectance values after the application of radiometric and geometric corrections (including orthorectification and spatial registration) (Sola et al., 2018).

Atmospheric correction of satellite data was conducted in order to develop a sufficiently reliable relationship between water quality variables and remote sensing data (Rozo et al., 2014; Bonansea et al., 2015). Atmospheric correction of Sentinel-2 imagery was performed using Sen2Cor module (version 2.5.5) within the Sentinel-2 Toolbox integrated in the Sentinel Application Platform software (SNAP), which is developed and freely distributed by ESA (ESA, 2018). Using Sen2Cor model each TOA Level-1C Sentinel-2 image was transformed into a Bottom-of-Atmosphere (BOA) Level-2A product (Steinhausen et al., 2018). Further details on Sen2Cor processor and its calibration can be obtained in Müller-Wilm (2016) and Richter et al. (2017). After atmospheric correction, RE1/2/3 bands and SWIR-1/2 bands were resampled to match de 10 m resolution of the other bands. Once preprocessing was complete, the normalized difference water index (NDWI) was used to mask out terrestrial features creating water-only images (McFeeters, 1996). The NDWI algorithm was used to delineate the reservoir surface on each image, while background information was restricted.

2.4. Model development

Once image processing was complete, atmospheric corrected values from MSI bands were used to develop relationships with measured SDT data using linear regression analysis, which is defined as a statistical technique used to relate a set of independent variables (BOA values of MSI bands) and a response variable (SDT measured in Río Tercero reservoir) by fitting a linear equation to the observed data (Jobson, 2012). The dataset used in this study was divided into two groups, a calibration subset (sampling campaigns performed on February 28, 2018; March 14, 2018; August 28, 2018; October 17, 2018) and a validation subset (sampling campaign performed on February 14, 2019; and March 24, 2019). The mean BOA reflectance value from a 3 × 3 grid centred on the GPS coordinates of the *in-situ* measurement sites was used to correlate with ground data. Based on previous studies, single band and band ratios were tested to ensure robust algorithms (Matthews, 2011). Using the calibration subset, algorithms to estimate SDT were generated using forward step-wise multiple regression analysis ($p < 0.05$). Standard regression assumptions were verified graphically and statistically. The Shapiro Wilks's test ($p > 0.05$) was used to prove assumption of normality. Levene's test ($p > 0.05$) was used to verify homogeneity of variances.

According to Matthews (2011) and Politi et al. (2015) researchers developed many different retrieval algorithms to estimate SDT, due to the fact that the best model varies from one reservoir to another according to water conditions. Thus, we chose not to employ preconceived models to estimate SDT and a wide variety of candidate algorithms were tested. Additionally, different goodness-of-fit measures, including the adjusted R-squared value (R^2), the bias (mean difference between estimated and observed SDT), and the root mean square error (RMSE) were calculated to obtain an estimate of the error associated with the estimations. The model with the greatest R^2 and the lowest Bias and RMSE was selected to retrieve SDT in the entire reservoir surface. The predictive capability of the model was also assessed by comparing the predicted and the observed SDT values of the validation subset by simple regression analysis. Finally, to assess water clarity in the reservoir, quantitative maps were created applying the selected model to the used imagery.

3. Results and discussion

3.1. Field data

The basic statistics of SDT measured in Río Tercero reservoir during the sampling campaigns are summarized in Table 2.

ANOVA did not showed significant differences between sampling campaigns ($p = 0.71$). However, this technique indicated significant differences when sampling sites were compared ($p > 0.01$). Sampling sites located in the western region of the reservoir (Sites 4 to 9) were significantly lower than those located in the eastern region (Sites 1, 2, 3, 10, and 11).

3.2. Algorithms

Regression model was performed using the calibration subset which contained 44 pairs of field and satellite data. Thus, measured SDT values were used to find the best combination of MSI spectral band or band ratios to estimate water clarity in Río Tercero reservoir. Eq. (1) shows the best model developed to predict SDT in the reservoir which included a combination of red edge and near infrared bands of MSI sensor ($R^2 = 0.86$):

$$SDT = 1.79 - 134.15{*}Band_{RE1} + 157.72{*}Band_{NIR} + 0.\,53{*}\left(\frac{Band_{RE3}}{Band_{NIRn}}\right) \tag{1}$$

where $Band_{RE1}$, $Band_{NIR}$, $Band_{RE3}$, and $Band_{NIRn}$ are the atmospherically corrected BOA values of MSI spectral bands.

Fig. 2 shows the comparison between field data and SDT values estimated by Sentinel-2 satellite. Fig. 2a, which represents comparison between observed and estimated SDT values used for model development, shows a good fit obtained from regression analysis ($R^2 = 0.85$, Bias = 0.03 m, and RMSE = 0.28 m) and a good agreement between the gradient and intercept of the regression line. The capacity of the generated algorithm was also validated comparing values of SDT measured in the field and SDT values predicted by applying the algorithm on BOA values of Sentinel-2 images of the validation dataset (Fig. 2b). In this case, the used goodness-of-fit measures also confirms the robustness and the high predictive capacity of the developed

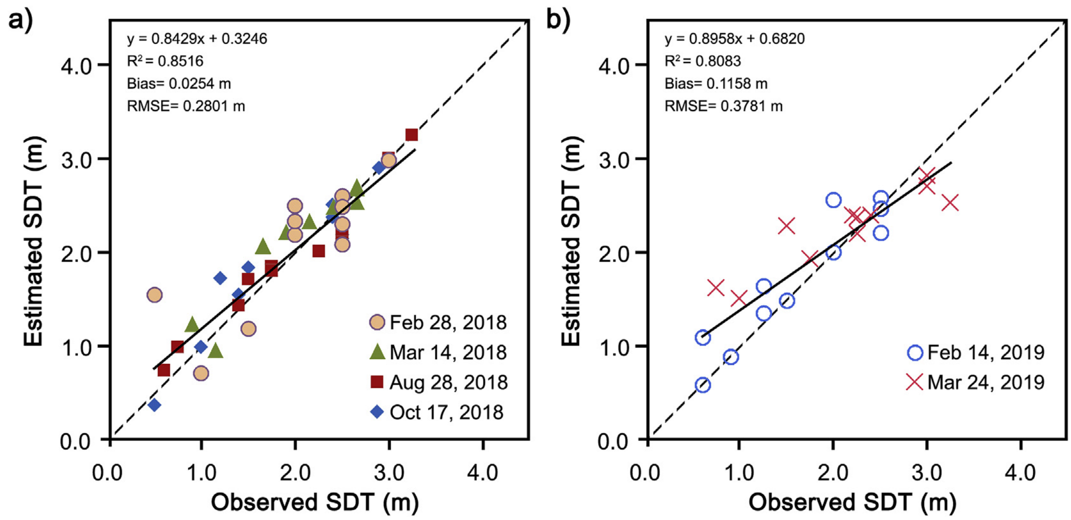

Fig. 2. Plots of observed versus estimated SDT values in Río Tercero reservoir with 1:1 fit line generated with a) calibration dataset and b) validation dataset.

algorithm and produce an acceptable error associated with the estimations (R^2 = 0.81, Bias = 0.12 m, and RMSE = 0.38 m).

Fig. 3 shows the spatial distribution of simulation mean errors during sampling campaigns. Comparing the mean difference between estimated and observed values of SDT, it was observed that the developed algorithm tended to generate a slight overestimation of SDT values when observed SDT values were low. On the other hand, when observed SDT values were high, the selected algorithm generated an underestimation of SDT values. This is evident in Fig. 3, which shows that in the western region of the reservoir, where lower values of water transparency were found, the overestimation of SDT values was evident by a positive difference between estimated versus observed SDT values. In the eastern region of the reservoir, the negative values of simulated errors demonstrated the underestimation generated by the used algorithm. Figure also shows that the central region of the reservoir presented the lower difference between estimated and observed water transparency values.

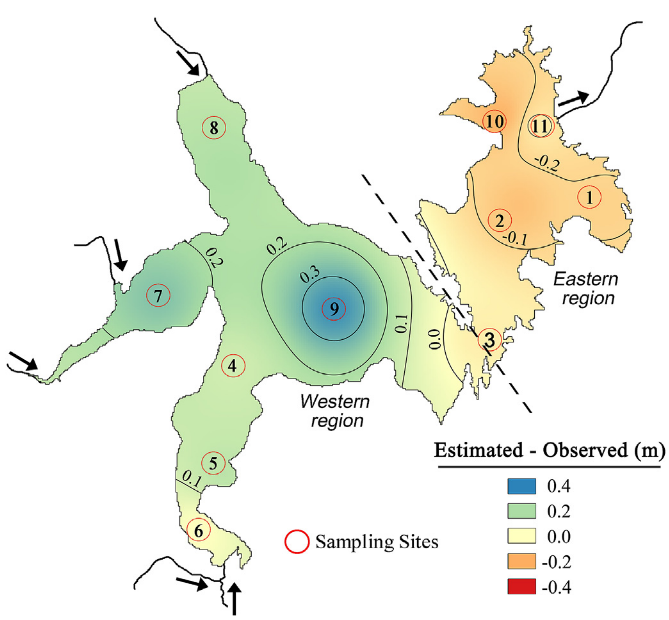

Fig. 3. Spatial distribution of mean difference between estimated versus observed SDT values in Río Tercero reservoir during sampling campaigns.

3.3. Algorithm implementation

As a real application of remote sensing techniques, the validated algorithm was applied to the used Sentinel-2 imagery obtaining a spatial representation of water clarity in Río Tercero reservoir during sampling campaigns (Fig. 4). This Figure shows that high-quality products can be derived from Sentinel-2 imagery. Coinciding with field data, satellite imagery shows a spatial patter of water clarity with lower values of SDT in the western region and increasing towards the eastern region of the reservoir. This longitudinal pattern could be associated with river runoff which delivers higher loads of suspended materials and dissolved solids into the western region of the reservoir that decrease the penetration of light and contribute to the reduction of water clarity. This situation is more evident close to river inputs. The opposite situation occurs in the eastern region of the reservoir where deeper waters and rapid sedimentation allow the measure of higher values of SDT. A similar spatial pattern of lower water clarity near river inflows and increasing with distance was found by Bonansea et al. (2015) in this reservoir and by Bazán et al. (2005), Giardino et al. (2010) and Guan et al. (2011) in different water bodies. Finally, as results show the generated algorithm could be used in the both Sentinel-2 satellites, thus the revisit time over the studied area could be reduced to 5 days, which is a benefit for operational uses and decision-making activities (Pahlevan et al., 2017; Sovdat et al., 2019).

Different multi-resolution satellites have been successfully used to estimate water clarity and other water quality variables of inland waters (Matthews, 2011; Villar et al., 2013; Dörnhöfer and Oppelt, 2016). However, as we have previously mentioned, there is an increasing international interest for the evaluation of the potential of new satellite systems and its derived products. In the present study, field data and Sentinel-2 imagery were used to generate a relevant and validated empirical algorithm for estimating and mapping water clarity in one of the most important reservoir of the central region of Argentina. Although we can confirm that the methodology used in the present study is adequate to estimate water clarity, it should be noted that the accuracy of the development algorithm is limited. Thus, for further validation, more simultaneous field observations with overpass time of Sentinel-2 must be compared for improving the accuracy and precision of the coefficients of the generated algorithm. Further, due to the influence of the nuclear power plant on water quality (Bonansea et al., 2015, 2018), we recommend that it must be taken into account when it is operative again for water quality assessment.

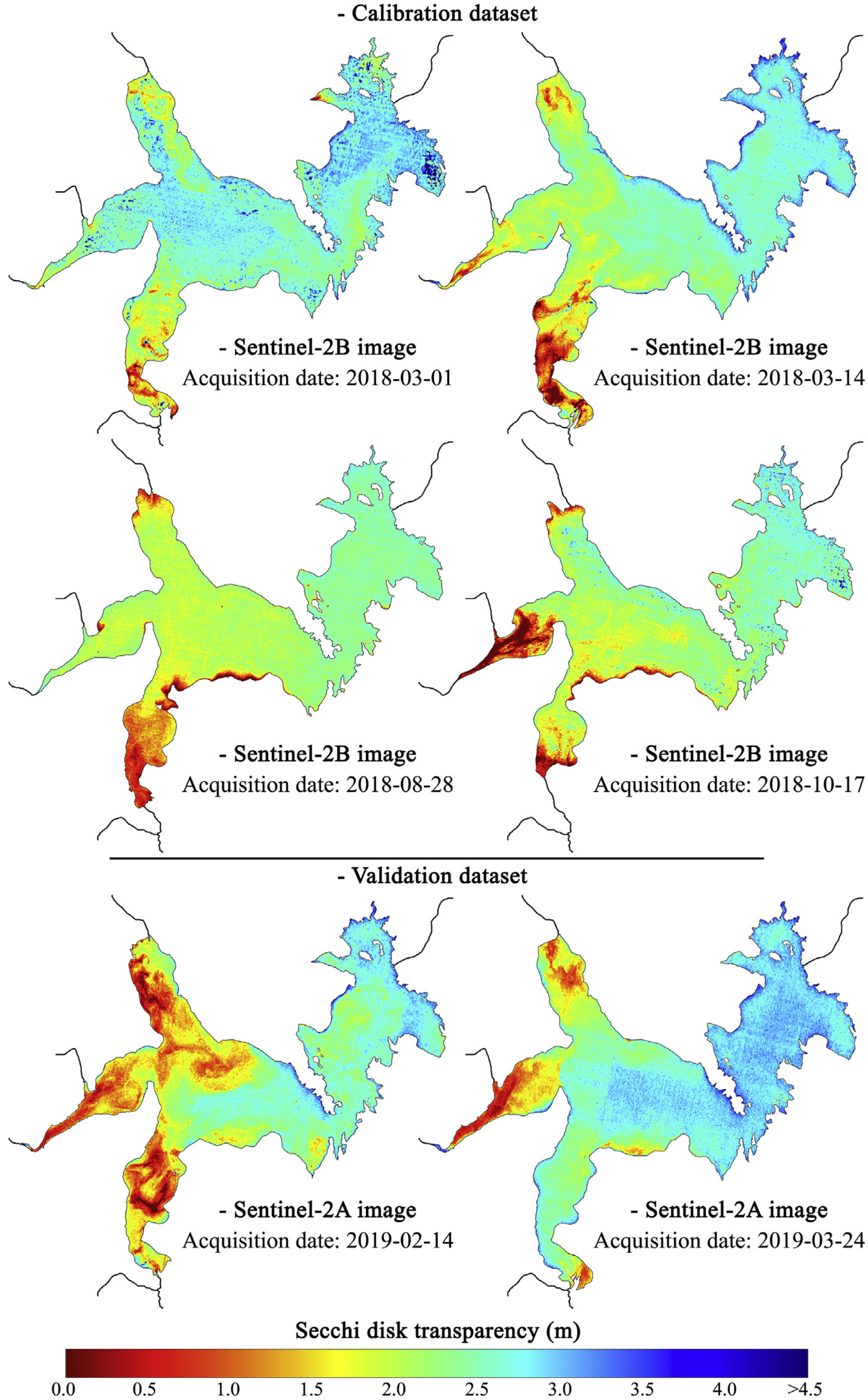

Fig. 4. Graphic representation of SDT in Río Tercero reservoir by applying Eq. (1) on atmospherically corrected values extracted from Sentinel-2 images.

4. Conclusions

This study demonstrates capabilities of Sentinel-2 mission to make a substantial contribution to the current assessment and understanding of aquatic systems by estimating and mapping a water quality characteristic in a reservoir of Argentina.

An algorithm to estimate SDT, a common measurement of water clarity, was generated and validated with high goodness-of-fit measures that confirms its robustness and its high predictive capacity ($R^2 = 0.81$, bias = 0.12 m, and RMSE = 0.38 m). Results also show that the produced water clarity maps enable for the interpretation of the behaviour of the variable in the whole reservoir. However, further research study with a larger data set is needed for a multi-temporal evaluation.

Acknowledgements

This study was supported by the CONICET and the Agencia Nacional de Promoción Científica y Tecnológica [grant number PICT-1408, 2015]; and SECyT-UNRC (Secretaría de Ciencia y Técnica, Universidad

Nacional de Río Cuarto) [grant number Res. 18A369, 2016]. The authors would like to thank Nautical Security Direction of Córdoba province for their collaboration in sampling campaigns.

Appendix A. Supplementary data

Supplementary data to this article can be found online at https://doi.org/10.1016/j.jsames.2019.102265.

References

Bazán, R., Corral, M., Pagot, M., Rodríguez, A., Oroná, C., Rodríguez, M., Larrosa, N., Cossavella, A., del Olmo, S., Bonfanti, E., Busso, F., 2005. Teledetección y modelado numérico para el análisis de la calidad de agua del embalse Los Molinos. Ing. Hidráulica México 20 (2), 121–135.
Bonansea, M., Rodriguez, M., Pinotti, L., Ferrero, S., 2015. Using multi-temporal Landsat imagery and linear mixed models for assessing water quality parameters in Río Tercero reservoir (Argentina). Remote Sens. Environ. 158, 28–41.
Bonansea, M., Ledesma, C., Rodriguez, M., 2016. Assessing the impact of land use and land cover on water quality in the watershed of a reservoir. Appl. Ecol. Environ. Res. 14 (2), 447–456.
Bonansea, M., Bazán, R., Ferrero, S., Rodríguez, C., Ledesma, C., Pinotti, L., 2018. Multivariate statistical analysis for estimating surface water quality in reservoirs. Int. J. Hydrol. Sci. Technol. 8 (1), 52–68.
Carlson, R., 1977. A trophic state index for lakes. Limnol. Oceanogr. 22 (2), 361–369.
Concha, J., Schott, J., 2016. Retrieval of color producing agents in Case 2 waters using Landsat 8. Remote Sens. Environ. 185, 95–107.
Dörnhöfer, K., Oppelt, N., 2016. Remote sensing for lake research and monitoring–Recent advances. Ecol. Indicat. 64, 105–122.
Drusch, M., Del Bello, U., Carlier, S., Colin, O., Fernandez, V., Gascon, F., Hoersch, B., Isola, C., Laberinti, P., Martimort, P., A.Meygret, A., Spoto, F., Sy, O., Marchese, F., Bargellini, P., 2012. Sentinel-2: ESA's optical high-resolution mission for GMES operational services. Remote Sens. Environ. 120, 25–36.
Du, Y., Zhang, Y., Ling, F., Wang, Q., Li, W., Li, X., 2016. Water bodies' mapping from Sentinel-2 imagery with modified normalized difference water index at 10-m spatial resolution produced by sharpening the SWIR band. Rem. Sens. 8 (4), 354.
El-Serehy, H., Abdallah, H., Al-Misned, F., Al-Farraj, S., Al-Rasheid, K., 2018. Assessing water quality and classifying trophic status for scientifically based managing the water resources of the Lake Timsah, the lake with salinity stratification along the Suez Canal. Saudi J. Biol. Sci. 25 (7), 1247–1256.
ESA, 2018. SNAP – ESA Sentinel Application Platform v6.0. http://step.esa.int/main/.
Ferral, A., Solis, V., Frery, A., Orueta, A., Bernasconi, I., Bresciano, J., Scavuzzo, C.M., 2017. Spatio-temporal changes in water quality in an eutrophic lake with artificial aeration. J. Water Land Dev. 35 (1), 27–40.
Giardino, C., Bresciani, M., Villa, P., Martinelli, A., 2010. Application of remote sensing in water resource management: the case study of Lake Trasimeno, Italy. Water Resour. Manag. 24 (14), 3885–3899.
González-Márquez, L., Torres-Bejarano, F., Torregroza-Espinosa, A., Hansen-Rodríguez, I., Rodríguez-Gallegos, H., 2018. Use of LANDSAT 8 images for depth and water quality assessment of El Guájaro reservoir, Colombia. J. South Am. Earth Sci. 82, 231–238.
Guan, X., Li, J., Booty, W., 2011. Monitoring lake Simcoe water clarity using Landsat-5 TM images. Water Resour. Manag. 25 (8), 2015–2033.
Jobson, J., 2012. Applied Multivariate Data Analysis: Volume II: Categorical and Multivariate Methods. Springer Science & Business Media.
Kloiber, S., Brezonik, P., Olmanson, L., Bauer, M., 2002. A procedure for regional lake water clarity assessment using Landsat multispectral data. Remote Sens. Environ. 82 (1), 38–47.
Mariazzi, A., Donadelli, J., Arenas, P., Di Siervi, M., Bonetto, C., 1992. Impact of a nuclear power plant on water quality of Embalse del Río Tercero reservoir (Córdoba, Argentina). Hidrobiologia 246, 129–140.
Matthews, M., 2011. A current review of empirical procedures of remote sensing in inland and near-coastal transitional waters. Int. J. Remote Sens. 32 (21), 6855–6899.
McFeeters, S., 1996. The use of normalized difference water index (NDWI) in the delineation of open water features. Int. J. Remote Sens. 17, 1425–1432.
Müller-Wilm, U., 2016. Sentinel-2 MSI – Level-2A Prototype Processor Installation and User Manual. Telespazio VEGA Deutschland GmbH, Darmstadt.
Olmanson, L., Bauer, M., Brezonik, P., 2008. A 20-year Landsat water clarity census of Minnesota's 10,000 lakes. Remote Sens. Environ. 112 (11), 4086–4097.
Olmanson, L., Brezonik, P., Finlay, J., Bauer, M., 2016. Comparison of Landsat 8 and Landsat 7 for regional measurements of CDOM and water clarity in lakes. Remote Sens. Environ. 185, 119–128.
Pahlevan, N., Sarkar, S., Franz, B., Balasubramanian, S., He, J., 2017. Sentinel-2 MultiSpectral Instrument (MSI) data processing for aquatic science applications: demonstrations and validations. Remote Sens. Environ. 201, 47–56.
Palmer, S., Kutser, T., Hunter, P., 2015. Remote sensing of inland waters: challenges, progress and future directions. Remote Sens. Environ. 157, 1–8.
Politi, E., Cutler, M., Rowan, J., 2015. Evaluating the spatial transferability and temporal repeatability of remote-sensing-based lake water quality retrieval algorithms at the European scale: a meta-analysis approach. Int. J. Remote Sens. 36 (11), 2995–3023.
Richter, R., Louis, J., Berthelot, B., 2017. Sentinel-2 MSI–level 2A Products Algorithm Theoretical Basis Document. https://earth.esa.int/c/document_library/get_file?folderId=349490&name=DLFE-4518.pdf.
Rozo, M., Nogueira, A., Castro, C., 2014. Remote sensing-based analysis of the planform changes in the Upper Amazon River over the period 1986–2006. J. South Am. Earth Sci. 51, 28–44.
Shang, S., Lee, Z., Shi, L., Lin, G., Wei, G., Li, X., 2016. Changes in water clarity of the Bohai Sea: observations from MODIS. Remote Sens. Environ. 186, 22–31.
Sola, I., García-Martín, A., Sandonís-Pozo, L., Álvarez-Mozos, J., Pérez-Cabello, F., González-Audícana, M., Llovería, R., 2018. Assessment of atmospheric correction methods for Sentinel-2 images in Mediterranean landscapes. Int. J. Appl. Earth Obs. Geoinf. 73, 63–76.
Sovdat, B., Kadunc, M., Batič, M., Milčinski, G., 2019. Natural color representation of Sentinel-2 data. Remote Sens. Environ. 225, 392–402.
Steinhausen, M., Wagner, P., Narasimhan, B., Waske, B., 2018. Combining Sentinel-1 and Sentinel-2 data for improved land use and land cover mapping of monsoon regions. Int. J. Appl. Earth Obs. Geoinf. 73, 595–604.
Traganos, D., Reinartz, P., 2018. Mapping Mediterranean seagrasses with Sentinel-2 imagery. Mar. Pollut. Bull. 134, 197–209.
Villar, R., Martinez, J., Le Texier, M., Guyot, J., Fraizy, P., Meneses, P., de Oliveira, E., 2013. A study of sediment transport in the Madeira River, Brazil, using MODIS remote-sensing images. J. South Am. Earth Sci. 44, 45–54.
Wang, Q., Atkinson, P., 2018. Spatio-temporal fusion for daily Sentinel-2 images. Remote Sens. Environ. 204, 31–42.
Wang, X., Zhang, F., Ghulam, A., Trumbo, A., Yang, J., Ren, Y., Jing, Y., 2017. Evaluation and estimation of surface water quality in an arid region based on EEM-PARAFAC and 3D fluorescence spectral index: a case study of the Ebinur Lake Watershed, China. Catena 155, 62–74.